Research Square

Preprints are preliminary reports that have not undergone peer review.
They should not be considered conclusive, used to inform clinical practice,
or referenced by the media as validated information.

Predicting the potential distribution of hemorrhagic fever with renal syndrome in Southwest China using the ecological niche modeling

Danjie Zhang
China Medical University
Zhiruo Zhu
China Medical University
Yanding Wang
LMU Munich
Linyuan Zhu
Air Force Medical University
Zitong Zheng
China Medical University
Ruidong Qu
China Medical University
Feng Shao
Air Force Medical University
Qiulan Chen
chenql@chinacdc.cn
China Centers for Disease Control and Prevention
Yuanyong Xu
Chinese PLA Center for Disease Control and Prevention
Wenyi Zhang
Chinese PLA Center for Disease Control and Prevention

Research Article

Keywords: Hemorrhagic fever with renal syndrome, Ecological niche modeling, MaxEnt, Southwest China, Risk assessment, Population density, Spatial heterogeneity.

Posted Date: March 24th, 2026

DOI: https://doi.org/10.21203/rs.3.rs-9153420/v1

License: This work is licensed under a Creative Commons Attribution 4.0 International License.
Read Full License

Additional Declarations: No competing interests reported.

Version of Record: A version of this preprint was published at Parasites & Vectors on September 1st, 2026. See the published version at https://doi.org/10.1186/s13071-026-07631-7.

Abstract

Background

Hemorrhagic fever with renal syndrome (HFRS) severely burdens China's public health. With its complex topography and rich biodiversity, Southwest China has historically incubated this natural focal disease. Currently, traditional environmental drivers of transmission here are increasingly eclipsed by anthropogenic forces, notably population agglomeration. Driven by these shifting dynamics, HFRS incidence and endemic ranges are expanding, yet systematic, regional-scale assessments remain scarce. Consequently, this study employs ecological niche modeling to map potential high-risk zones. Ultimately, we aim to explore the core mechanisms driving HFRS prevalence amid the complex interplay of natural environments and human activities.

Methods

Surveillance data of HFRS cases in Southwest China from 2014 to 2023 were obtained from the China Information System for Disease Control and Prevention (CISDCP). A Maximum Entropy (MaxEnt) model was constructed by integrating occurrence records with multisource environmental variables, including meteorological, socioeconomic, and land cover factors. Model performance was evaluated using the Area Under the Curve (AUC) of the Receiver Operating Characteristic (ROC), and the Jackknife test was employed to quantify the contribution of each variable.

Results

The MaxEnt model demonstrated robust predictive performance with a mean AUC of 0.902. Population density was identified as the predominant predictor (73.5% contribution), followed by the Normalized Difference Vegetation Index (NDVI) in May (9.2%) and annual mean temperature (5.8%). The spatial distribution of risk exhibited a core aggregation with sporadic dispersion pattern, with high-risk zones concentrated in the Chengdu-Chongqing urban agglomeration and localized clusters in Yunnan Province. Response curves revealed a sigmoidal positive correlation between population density and disease risk. Meteorological factors, such as temperature and precipitation, exhibited non-linear inverted U-shaped or U-shaped relationships, constraining the spatial boundaries of transmission.

Conclusions

The spatial heterogeneity of HFRS in Southwest China is jointly driven by anthropogenic activities and natural environmental constraints. Human population density acts as the primary amplifier of transmission risk, supporting the human behavior amplification effect in natural focal diseases. These

findings suggest a strategic shift from blanket prevention to precision control, prioritizing active surveillance in densely populated urban fringes and areas undergoing infrastructure development.

Background

Hemorrhagic fever with renal syndrome (HFRS) is a natural focal disease caused by hantavirus infection, characterized primarily by acute onset, rapid disease progression, and a high mortality rate[1, 2]. China is one of the countries most severely affected by HFRS globally[3, 4]. Since the 1980s, the annual reported case count exceeded 100,000 for many years, placing a sustained and significant burden on the public health system[5, 6]. Although the national HFRS incidence rate in China has declined significantly in recent years following the implementation of comprehensive control measures—such as vaccination, reservoir host control, and health education—this trend does not indicate that epidemic risk has been eliminated, given the continued occurrence of sporadic cases and localized clusters[7, 8]. Notably, the epidemiological pattern of HFRS is not static but rather undergoes continuous evolution, driven by the interplay of natural environmental and socioeconomic factors[9, 10].

Particularly in the context of global warming, alterations in temperature and precipitation patterns can indirectly modulate hantavirus transmission risk by influencing the population dynamics and habitat distribution of reservoir hosts such as rodents[11, 12],thereby driving a geographical shift in high-risk areas[7, 10]. Against this backdrop, the epidemiological pattern of HFRS, traditionally predominant in northern regions, is currently exhibiting new characteristics of spatial variation[7, 9]. In recent years, the epidemiological dynamics of HFRS in Southwest China have attracted increasing attention due to rising incidence and the region's unique ecological landscape. While traditional high-incidence areas have long been concentrated in Northeast China and the North China Plain[13], Southwest China has recently exhibited an upward trend in reported cases and a gradual expansion of the endemic range, emerging as a potential high-risk region that warrants attention within the national prevention and control framework[14–16].

The study area is characterized by complex topography, featuring the coexistence of plateaus, mountains, and basins, diverse climatic types, and significant ecological heterogeneity; consequently, its natural conditions differ markedly from traditional HFRS-endemic areas[17]. This unique physiographical and climatic context may result in distinct reservoir species compositions, transmission pathways, and environmental drivers compared to the northern endemic areas, thereby shaping a region-specific pattern of HFRS transmission[18–20]. Previous studies have demonstrated that meteorological factors, socioeconomic factors, and land cover variables are closely associated with the occurrence of HFRS[21]. However, existing literature has largely concentrated on specific HFRS-endemic cities in southwestern China, with a primary emphasis on analyzing demographic characteristics and the spatiotemporal dynamics of the epidemic[19, 22–24]. Consequently, systematic and quantitative assessments regarding the distributional characteristics of HFRS risk factors and projected risk patterns at a holistic regional scale remain insufficient[7]. Given these limitations, it is imperative to conduct a comprehensive analysis of multidimensional influencing factors at a broader spatial scale. Therefore, this study aims to

systematically identify the combined effects of meteorological, socioeconomic, and land cover variables on the occurrence of HFRS in southwestern China, delineate potential disease risk zones, and quantify the population exposed to varying levels of risk, thereby providing a scientific basis for comprehensively assessing the associated public health burden and formulating region-specific prevention and control strategies.

Methods

HFRS surveillance data

Surveillance data regarding HFRS cases in Southwest China spanning from 2014 to 2023 were sourced from the Infectious Disease Reporting System of the Chinese Center for Disease Control and Prevention (China CDC). All reported cases were confirmed strictly following the standardized diagnostic criteria formulated by the national CDC[25].

Base map and population data

The base map was obtained from the National Platform for Common Geospatial Information Services (https://www.tianditu.gov.cn/; Map Approval No. GS(2024)0650), featuring polygon vector layers for provincial, prefectural, and county-level administrative divisions. Population data for southwestern China were derived from the Seventh National Population Census conducted in 2020, accessed via the National Bureau of Statistics of China (https://www.stats.gov.cn/sj/pcsj/rkpc/7rp/zk/indexce.htm). Population density was calculated by dividing the population size by the land area of each county.

Environmental variables

To investigate the environmental risk factors influencing the spatiotemporal distribution of HFRS in recent years, we collected data on a range of environmental variables, including meteorological factors and land cover. The selection of these variables was informed by prior studies and expert consultation regarding their potential impact on the spatiotemporal variation of the HFRS epidemic.

Meteorological data for southwestern China spanning from 2014 to 2023 were obtained from the China Meteorological Data Service Centre (https://data.cma.cn/). The meteorological variables included in this study comprised the multi-year mean relative humidity, multi-year mean temperature, and multi-year mean precipitation. Using ArcGIS 10.8 software (ESRI, Redlands, CA, USA), raster layers representing the mean meteorological data for the 2014–2023 period were generated via the Kriging interpolation method.

Elevation data were derived from a nationwide Digital Elevation Model (DEM) with a spatial resolution of 1 km × 1 km, obtained from the National Earth System Science Data Center

(http://www.geodata.cn/data/datadetails.html?dataguid=201519481253546&docid=1301). Additionally, slope and aspect variables were calculated from the elevation data using ArcGIS 10.8 software.

Land use data for the year 2013 were obtained from the National Earth System Science Data Center (https://www.geodata.cn/), provided as a raster layer with a spatial resolution of 1 km × 1 km.

Data for the Normalized Difference Vegetation Index (NDVI) were obtained from the National Tibetan Plateau Data Center (https://www.tpdc.ac.cn/). As the most widely used vegetation index, NDVI indicates vegetation growth status and coverage, thereby comprehensively reflecting the environmental conditions of the region.

All environmental variable datasets were projected to a unified geographic coordinate system and converted into raster format. Subsequently, the data were resampled to a consistent spatial resolution of 1 km and clipped to the extent of the study area using vector boundary data in ArcGIS 10.8.

Study area

Southwestern China is located between approximately 97°21'–110°11' E and 21°08'–34°19' N, situated at the eastern margin of the Qinghai-Tibet Plateau and encompassing the main body of the Yunnan-Guizhou Plateau. The region covers a total area of approximately 1.14 million km² (Fig. 1). The region exhibits diverse climatic types, predominantly characterized by a subtropical monsoon climate alongside features of a plateau mountain climate. The mean annual temperature ranges from 8 to 20°C, with annual precipitation typically falling between 800 and 1800 mm. Notably, significant vertical climate differentiation is observed in local alpine valley areas[17]. According to the 2021 provincial statistical yearbooks and data from the Seventh National Population Census, the permanent resident population totaled approximately 198 million by the end of 2020. The population distribution is characterized by relative concentrations in basins, plains, and urban areas, in contrast to the sparsely populated mountainous regions.

Statistical methods

Prior to model construction, to ensure the robustness and interpretability of the analytical results, we constructed an initial set of variables by systematically reviewing existing literature to screen for potential environmental factors associated with the occurrence of HFRS. All candidate variables were entered into the MaxEnt model for a preliminary run, with the number of replicates set to 1. The Jackknife test was subsequently employed to evaluate the contribution and importance of each variable to the model. To prevent model overfitting and potential interference with result interpretation caused by the coexistence of highly correlated variables, we subsequently conducted a multicollinearity test using Spearman's rank correlation analysis, establishing a threshold of 0.8 ($|r| \geq 0.8$)[26]. For pairs of highly correlated variables, selection was prioritized based on contribution metrics derived from the preliminary model run: the variable with the higher contribution was retained, while the lower-contributing variable

was excluded. Ultimately, a final set of variables that were mutually independent and possessed significant explanatory power for HFRS transmission risk was selected to construct the final model.

Maximum entropy modeling process

Model construction

In this study, the Maximum Entropy (MaxEnt, version 3.4.3) model was employed for ecological niche modeling. Based on the principle of maximum entropy, this model predicts the probability of presence in specific habitats by integrating geographic occurrence records of HFRS cases with environmental background points; it is widely recognized as a robust machine learning method characterized by high predictive accuracy[27, 28].

Model training and parameter optimization:

To construct a high-precision predictive model, the key eco-environmental factors identified during the screening process were incorporated into the MaxEnt model. In terms of data partitioning, 75% of the HFRS occurrence records were randomly selected as the training set for model calibration, while the remaining 25% were reserved as the test set for model validation[29, 30].

To minimize random errors associated with single simulations and enhance the stability of the results, the model was executed with 10 replicates, and the final output was derived from the average of these 10 runs. Apart from these specific settings, all other parameters were maintained at the software's default values[31].

Model performance evaluation:

The predictive performance of the model was evaluated primarily using the Receiver Operating Characteristic (ROC) curve and the Area Under the ROC Curve (AUC)[32]. The AUC values range from 0 to 1, with a value closer to 1 indicating superior predictive performance. Specifically, an AUC of 0.5 represents a random prediction. The performance levels are categorized as follows: 0.5–0.6 is considered poor; 0.7–0.8 is fair; 0.8–0.9 is good; and 0.9–1.0 is excellent[33]. Furthermore, a threshold-dependent binomial test was employed, utilizing the omission rate as a test statistic to comprehensively evaluate the statistical significance of the model and assess the potential for overfitting[34].

Analysis of environmental variable importance

To identify the key driving factors influencing the distribution of HFRS, the Jackknife test was employed to quantitatively evaluate the contribution of each environmental variable to the model gain, thereby identifying the dominant variables containing the most critical information[35].Additionally, response curves were utilized to analyze the non-linear response patterns of the predicted probability of HFRS

occurrence to variations in individual variables, thereby elucidating the quantitative relationships between environmental factors and disease risk[34, 36].

Risk zonation and population exposure assessment

The output of the MaxEnt model consists of continuous probability values ranging from 0 to 1, representing the environmental suitability for the occurrence of HFRS (i.e., the potential risk). Based on the characteristics of the probability distribution, the risk levels were stratified into three categories: low-risk zones (≤ 0.29), medium-risk zones (0.29–0.45), and high-risk zones (> 0.45). Finally, a spatial overlay analysis was performed using ArcGIS software to integrate the reclassified risk zonation map with population raster data. This process allowed for the quantitative estimation of the size and spatial distribution characteristics of the population exposed to varying risk levels at both the prefectural and regional scales[37].

Results

Descriptive analysis results

The mean annual incidence rate in Southwestern China was 0.19 per 100,000 population, with the rate reaching 0.32 per 100,000 in 2023. Furthermore, HFRS cases exhibited pronounced seasonal fluctuations, characterized by a primary peak during the spring-summer period (April–June) and a secondary peak during the autumn-winter period (November–January). In terms of geographic distribution, the Liangshan Yi Autonomous Prefecture in Sichuan Province, along with the Dali Bai Autonomous Prefecture and Chuxiong Yi Autonomous Prefecture in Yunnan Province, were identified as the primary high-incidence areas. Collectively, these three regions accounted for 62.60% of the total cases reported in Southwestern China. Demographic analysis indicated that males and farmers aged 20–60 years constituted the primary high-risk groups. The incidence rate among males was 45.01 per 100,000 population, significantly exceeding that among females (1.76 per 100,000 population). Furthermore, significant heterogeneity in incidence rates was observed across prefecture-level cities, with cases predominantly concentrated in mountainous regions and ethnic autonomous prefectures.

Correlation between risk factors and HFRS cases

The results of the correlation analysis are presented in Fig. 2. Based on the modeling results, key ecological environmental variables influencing HFRS transmission risk—including monthly mean Normalized Difference Vegetation Index (NDVI) (specifically for May and August, with a cumulative contribution of 10.4%), land use (specifically 2013 data, 3.1%), annual mean temperature (0.5%), annual precipitation (1.9%), population density (utilizing 2020 data, 69.2%), annual mean relative humidity (4.1%), and slope (1.1%)—were selected to construct the predictive model for HFRS transmission risk in the southwest region.

Model Evaluation

The close proximity between the average omission rate of the test data and the predicted omission rate indicated that the trained model was statistically significant; furthermore, the mean Area Under the Curve (AUC) value for 10 replicate runs was 0.902 (Standard Deviation [SD] = 0.017), demonstrating that the MaxEnt model exhibited high predictive sensitivity and accuracy with robust performance.(Figs. 3–5)

Key predictive variables for HFRS

The relative contribution analysis based on the MaxEnt model revealed significant differences in the explanatory power of various variables regarding the spatial distribution of Hemorrhagic Fever with Renal Syndrome (HFRS).Specifically, population density, the Normalized Difference Vegetation Index for May (NDVI5), and annual mean temperature were identified as the top three predictors in the model, with relative contributions of 73.5%, 9.2%, and 5.8%, respectively, accounting for a cumulative contribution of 88.5%. Furthermore, results from the Jackknife test confirmed that population density yielded the highest model gain when used in isolation. Response curve analysis further elucidated the non-linear relationships between key variables and the probability of HFRS occurrence. Specifically, population density demonstrated a significant positive correlation with HFRS risk, and its response curve exhibited a typical sigmoidal or threshold growth pattern: in the low-density range, the probability of occurrence rose exponentially with increasing population; once population density reached approximately 2500 people/km², environmental suitability rapidly ascended to high values, maintaining a probability above 0.65, and plateaued at a high level beyond approximately 19,000 people/km². Regarding vegetation factors, the response trends for both NDVI5 and the Normalized Difference Vegetation Index for August (NDVI8) exhibited an overall negative relationship, indicating that the probability of HFRS occurrence generally declined with increasing vegetation coverage. However, within specific value ranges, these indices still indicated environments relatively suitable for disease occurrence; specifically, the response values for NDVI5 were primarily concentrated within the range of 0.1–0.8, while those for NDVI8 were distributed between 0.25 and 0.75.

The response curves for meteorological factors revealed a distinct bimodal relationship between relative humidity and the probability of HFRS occurrence, with predicted peaks observed at approximately 65% and 82%.Annual mean precipitation exhibited a typical U-shaped relationship with the probability of HFRS occurrence, with the lowest predicted risk observed in the range of approximately 1210–1640 mm; in contrast, annual mean temperature showed an inverted U-shaped relationship, peaking within the 10–16°C interval.lope exhibited an overall weak inverted U-shaped relationship with the probability of HFRS occurrence, reaching a relative high in predicted risk at approximately 17–23.5°, with a corresponding response probability of 0.7–0.8. Analysis of land cover types indicated that impervious surfaces and forests were associated with the highest HFRS occurrence probabilities, followed by cropland and shrubland, whereas grassland and water bodies exhibited relatively lower predicted risks.(Fig. 6)

Risk of HFRS occurrence:

Figure 7 illustrates the spatial heterogeneity of the potential HFRS risk in Southwest China as predicted by the MaxEnt model. The results indicated that the distribution of HFRS within the study area exhibited significant spatial clustering characteristics. Based on the reclassification standards, the study area was dominated by low-risk areas, covering 91.0% of the total area; whereas high- and medium-risk areas accounted for 3.0% and 6.0%, respectively. Table 1 further quantifies the exposed areas and the size of the population at risk within different administrative units across each risk level. The high-risk areas exhibited a spatial distribution pattern characterized by "core aggregation with sporadic dispersion." The primary cluster was situated in the northeastern part of the study area (specifically, the Sichuan Basin and its vicinity), encompassing densely populated urban agglomerations such as the main urban districts of Chongqing, Chengdu, Deyang, Mianyang, and Nanchong. Furthermore, significant high-risk areas with a punctuate distribution and weak spatial continuity were identified in Yunnan Province in the southwestern region, predominantly concentrated in the central part of Dali Bai Autonomous Prefecture, Chuxiong Yi Autonomous Prefecture, and parts of Baoshan City. The medium-risk areas are predominantly distributed in annular or band-like patterns along the periphery of high-risk zones, forming an ecotone that transitions from high-risk to low-risk areas. These regions are concentrated in the peripheral extension zones of the Chengdu-Chongqing urban agglomeration, as well as in Chuxiong Yi Autonomous Prefecture and Yuxi City in central Yunnan Province. In contrast, low-risk areas extensively cover the western and southern margins of the study area, particularly in higher-elevation regions such as Ganzi Tibetan Autonomous Prefecture, Aba Tibetan and Qiang Autonomous Prefecture, and the southern part of Pu'er City. (Fig. 7)

Table 1
Definitions and types of environmental variables

Variable classification	Variable name	Definition	Resolution	Variable type
Climatic	MAT	Annual Mean Temperature	1km	Continuous
	AAP	Annual Average Precipitation	1km	Continuous
	RH	Average Annual Relative Humidity	1km	Continuous
Geographical	LD	Land Cover	1km	Categorical
	DEM	Digital Elevation Model	1km	Continuous
	Aspect	Terrain Aspect	1km	Continuous
	Slope	Terrain Slope	1km	Continuous
	NDVI3	Normalized Difference Vegetation Index in March	1km	Continuous
	NDVI5	Normalized Difference Vegetation Index in May	1km	Continuous
	NDVI7	Normalized Difference Vegetation Index in July	1km	Continuous
	NDVI8	Normalized Difference Vegetation Index in August	1km	Continuous
	NDVI9	Normalized Difference Vegetation Index in September	1km	Continuous
Socioeconomic	DP	Density of population	1km	Continuous

Discussion

Based on HFRS case data from Southwest China spanning 2014–2023, this study utilized the Maximum Entropy (MaxEnt) model to systematically characterize potential high-risk zones and key environmental drivers of hemorrhagic fever with renal syndrome (HFRS), effectively bridging the knowledge gap regarding the lack of systematic, quantitative risk assessments at a holistic regional scale in this region[38].

The results indicate robust model performance, with HFRS incidence risk exhibiting significant spatial heterogeneity at the regional scale[39]; high-risk zones are not uniformly distributed but are concentrated in areas characterized by prominent interactions between specific ecological conditions and human activities, revealing the spatial patterns where the natural environment and human exposure co-drive disease transmission. Concurrently, natural environmental variables, such as vegetation indices and temperature, demonstrated significant threshold effects, delineating suitable habitats for reservoir host

survival and viral transmission. Spatially, the study identified a risk pattern characterized by higher density in the north versus sparsity in the south, featuring the coexistence of core clustering and multi-point sporadic occurrences[40]. Specifically, it confirmed a contiguous high-risk zone anchored by the Chengdu-Chongqing urban agglomeration, along with localized sporadic risk patches in regions such as Yunnan.

The results indicate that population density was the predominant predictor, yielding the highest percent contribution to the model and exhibiting the highest independent gain in the jackknife test. This finding suggests that in the topographically complex Southwest China, the intensity of human activity and the degree of population aggregation are critical determinants of the spatial heterogeneity of HFRS distribution. This conclusion aligns closely with findings from numerous recent studies conducted in mainland China, as well as in other high-incidence regions such as Northeast and East China[41, 42]. For instance, Wang et al., analyzing 34 years of surveillance data in China, demonstrated that population aggregation driven by urbanization is significantly and positively correlated with HFRS transmission dynamics; notably, in rapidly developing small- and medium-sized cities, the explanatory power of demographic factors regarding disease distribution often surpasses that of climatic variables alone[42].

The response curves in this study reveal that the probability of HFRS occurrence follows a characteristic sigmoidal non-linear increase with rising population density, reaching high-risk levels after surpassing a specific threshold. This finding substantiates the pronounced "human behavior amplification effect on natural focal diseases" in densely populated areas. This aligns with the review by Li et al. regarding the urbanization risks of HFRS, which noted that densely populated areas are often characterized by habitat fragmentation in the urban-rural fringe, creating environments particularly conducive to the survival and proliferation of commensal rodent hosts such as *Rattus norvegicus*[43].

Furthermore, a study published by Zhang et al. revealed that with the increase in urbanization rates in China, *Rattus norvegicus*-dominated foci are gradually replacing *Apodemus agrarius*-dominated sylvatic foci as the primary source of transmission risk. This shift explains why the high-density urban areas in our study exhibited sustained high suitability[44]. Notably, although some previous studies have suggested that high levels of urbanization may reduce rodent density due to improved infrastructure and increased impervious surfaces, thereby presenting an "inverted U-shaped" risk trend[43]. This discrepancy may be attributed to the unique "mountainous urbanization" pattern in Southwest China, where urban expansion typically proceeds along river valleys or intermontane basins; consequently, human settlements are closely interspersed with surrounding natural ecosystems such as farmland and forests, lacking distinct geographical buffer zones.

Furthermore, a study by Liu et al. suggested that population density serves not only as a proxy for host exposure opportunities but also reflects the aggregation effect of floating populations (e.g., rural-to-urban migrant workers). These groups often reside in "urban villages" or near construction sites characterized by relatively poor sanitary conditions, which increases the frequency of contact with

infected rodents and their excreta, thereby sustaining continuous transmission risk in high-density areas[42, 43].

In this study, the responses of NDVI5 and NDVI8 to the spatial distribution of HFRS generally exhibited a negative trend; however, within specific ranges characterized by moderate levels of vegetation coverage, the risk of disease occurrence was relatively high. This nonlinear response pattern suggests that, driven by a trade-off between survival resources and contact opportunities, the transmission risk of HFRS typically peaks in areas characterized by intermediate vegetation density, such as cultivated lands and shrublands, rather than in primary forests with the highest vegetation density. This finding is consistent with the conclusions of recent studies conducted by Liu et al. and Xiang et al. in other regions of China[45].This may be attributed to two mechanisms: first, the geographical constraints on human activities. In the southwest region, extremely high NDVI values typically correspond to remote, high-altitude dense forests or nature reserves with minimal human presence. According to Yuan et al., although such habitats are suitable for the survival of certain wild rodents, the high degree of isolation from human populations effectively breaks the rodent-to-human transmission chain, thereby resulting in a low transmission risk[46].

Second, the dilution effect of biodiversity. Research by Zheng et al. suggests that in areas with high vegetation coverage and rich biodiversity, competition from non-host species may suppress the population density of specific hantavirus hosts, thereby acting as an ecological barrier[47].Furthermore, this study observed a high temporal coincidence between NDVI5 and the primary epidemic peak in spring and summer. Consistent with the recent findings by Liu et al. regarding the environmental drivers of HFRS in China, spring and summer represent the period of most intensive agricultural activity in the southwest region (e.g., harvesting and sowing), thereby increasing the likelihood of human exposure to rodents and their excreta (aerosols) during field operations[48].

In contrast to NDVI5, NDVI8 exhibited a significant lagged effect on HFRS, primarily driving the formation of the secondary epidemic peak in autumn and winter[49]. Zhang et al. indicated that there is a time lag of approximately 3–5 months in the regulation of rodent populations by vegetation[50].High NDVI in August signifies an abundant food supply in the ensuing autumn, which facilitates the proliferation of rodent populations to their annual peak between October and November. Subsequently, declining temperatures and diminishing food resources in winter drive these high-density wild rodent populations to migrate toward human settlements for indoor overwintering, thereby triggering the epidemic peak observed from November to the following January[51].

Climatic and meteorological factors serve as critical determinants in the occurrence and spread of natural focal diseases; however, their underlying mechanisms are highly complex, and research findings regarding the impact of individual climatic variables on virus transmission have varied across different geographical regions[52, 53]. This study identified an inverted U-shaped relationship between mean temperature and the probability of HFRS occurrence, with peak risks observed within the range of 10–16°C. Rising temperatures facilitate the growth of crops and natural vegetation, providing abundant food

resources and shelter for reservoir rodents (predominantly *Rattus norvegicus*). This consequently enhances rodent population density and activity frequency, further increasing the likelihood of human-rodent contact and ultimately elevating the risk of infection.

Research by Zhang et al. indicated that mild temperatures (10–20°C) significantly enhance the survival rates of juvenile rodents and the pregnancy rates of adults; simultaneously, this temperature range is optimal for crop growth, thereby providing abundant food resources for the rodent population[50].Excessively low or high temperatures may inhibit host activity or alter human behavioral patterns, thereby reducing transmission risk. As elucidated by Liu et al., high summer temperatures (> 25°C) not only induce heat stress responses in rodents, restricting their foraging activities, but also reduce the duration of human outdoor agricultural activities, thereby decreasing the frequency of human-rodent contact[54].

Precipitation exhibited a distinct U-shaped relationship with HFRS in the study area, characterized by the lowest risk within the intermediate precipitation range, whereas risks were elevated under extreme conditions of both low and high precipitation. As indicated by Xiang et al., during periods of precipitation deficit, the scarcity of food and water resources in natural habitats drives wild rodents to migrate toward human settlements, particularly granaries and kitchens. This “commensal” behavior significantly increases the risk of indoor infection, while the resurgence of risk at extremely high precipitation levels may be attributed to flood disasters that compel the migration of rodent communities[55].

However, the lowest risk observed within the intermediate precipitation range may reflect an ecological counter-balancing mechanism driven by the synchronization of rain and heat characteristic of the southwest region. Within this interval, despite favorable vegetation growth, sustained rainfall may lead to the inundation of rodent burrows or trigger an explosive proliferation of ectoparasites (e.g., gamasid mites) on juvenile rodents under high-humidity conditions, thereby increasing mortality rates. As suggested by certain regional studies, moderate moisture paradoxically limits the explosive expansion of host population density[56].

The bimodal distribution of relative humidity reveals a dual dependency of virus transmission on environmental moisture. On the one hand, moderate ambient humidity facilitates the suspension and survival of virus-laden aerosols; on the other hand, high humidity is frequently coupled with region-specific agricultural cycles. Notably, while laboratory evidence suggests that humid environments prolong the *in vitro* half-life of hantaviruses, in the context of real-world epidemiology, the extremely high humidity in the southwest region is frequently accompanied by high temperatures. This hot and humid combination is detrimental to the long-term stability of lipid-enveloped viruses[57–59].

In summary, the influence of meteorological factors in the southwest region is not exerted through a simple unidirectional linear mechanism but is instead jointly mediated by ecological behavioral pathways such as drought-induced migration and optimal-temperature breeding. This implies that when developing early warning strategies, in addition to focusing on rodent control during the rainy season, greater emphasis should be placed on indoor rodent eradication and preventive measures during the dry season.

This finding stands in marked contrast to the majority of studies focusing on the plains regions of China (e.g., the Guanzhong Plain and the Northeast China Plain). Previous research generally suggests that flat terrain with a slope of less than 10° is conducive to mechanized cultivation and irrigation, thereby representing areas characterized by the highest rodent density and the most frequent human-rodent contact[60, 61]. However, the skewing of risk towards intermediate slopes observed in this study may be attributed to the unique vertical agriculture and mountainous settlement patterns in the southwest region. Due to the scarcity of flat terrain resources, extensive agricultural activities (e.g., terraced fields and drylands) and rural settlements are compelled to extend onto the hillsides[62]. According to a study by Yang et al. on the distribution of traditional villages in the southwest region, a substantial number of settlements are situated on gentle to intermediate slopes. This terrain not only facilitates natural drainage and prevents waterlogging but also falls precisely within the suitable nesting habitat range of wild rodents, such as *Apodemus agrarius*[63, 64].

Therefore, moderate slope zones effectively constitute a unique "human-rodent-environment" interface specific to the southwest mountainous regions, rather than acting as geographical barriers. In terms of land cover types, this study identified that impervious surfaces and woodlands exhibited the highest probability of HFRS occurrence. The elevated risk associated with impervious surfaces underscores the role of rapid urbanization in driving HFRS transmission; notably, a recent study by Xiang et al., based on 34 years of surveillance data in China, indicated that the expansion of impervious surfaces has superseded certain natural factors, emerging as the primary predictor variable for HFRS transmission[65].This is primarily attributed to the fact that urbanization in the southwest region is often accompanied by the persistence of urban villages and aging residential neighborhoods; characterized by suboptimal sanitation, these areas are prone to harboring commensal rodent-borne foci dominated by *Rattus norvegicus*. A review by Li et al. further emphasizes that the expansion of impervious surfaces during urbanization effectively provides stable shelters for commensal rodents by modifying microhabitats (e.g., sewers and refuse accumulation sites), thereby prolonging viral transmission chains within anthropogenic environments[66]. Furthermore, the elevated risk associated with woodlands elucidates the characteristics of mixed-type foci within the region. In contrast to the distinct separation between urban areas and forests observed in the northern plains, mountainous cities in the southwest often exhibit a mosaic landscape described as cities within forests and houses within mountains. This ecotone, resulting from the high proximity between woodlands and residential zones, significantly increases the probability of residents (particularly peripheral farmers) encountering wild rodent hosts—primarily *Apodemus agrarius* inhabiting forest edges—during foraging or agricultural activities. Consequently, the dual high risk attributed to both impervious surfaces and woodlands in this study substantively reflects the complex reality of the spatial overlap and interplay between commensal and wild rodent-borne foci in the southwest region.

In addition to natural and conventional socioeconomic determinants, the potential impact of large-scale infrastructure development—such as the construction of highways and water conservancy hubs—on the transmission risk of HFRS cannot be overlooked. Such high-intensity anthropogenic disturbances alter land cover and hydrological characteristics, thereby directly inducing the fragmentation and restructuring

of rodent habitats. Taking the Three Gorges Project as a case in point, long-term ecological monitoring has demonstrated that water impoundment in the reservoir area has precipitated a significant insularization effect[67]. As water levels rise periodically, the resulting inundation of low-elevation habitats compels reservoir hosts, such as *Rattus norvegicus*, to undergo a forced migration toward unsubmerged islands or peripheral high-altitude agricultural zones; this displacement precipitates an acute, short-term surge in local rodent density, thereby intensifying interspecific competition and accelerating the turnover of dominant species[68, 69]. Similarly, in the context of large-scale infrastructure development recently undertaken in Yunnan Province—particularly water conservancy projects—rodents may be driven to migrate toward construction camps or surrounding residential areas in search of foraging resources and new habitats[19, 23, 70, 71]. This process significantly amplifies the likelihood of human exposure to infected hosts and their excreta, highlighting the critical need to prioritize the prevention of emergent infectious foci triggered by drastic ecological transformations, particularly during the construction phase and within resettlement areas.

This study is subject to certain limitations: First, since case data were derived from a passive surveillance system, there is a potential for underreporting bias stemming from mild clinical presentations or insufficient health-seeking behavior among patients, which may, to a certain extent, lead to an underestimation of the true incidence. Second, given that this study was conducted as an ecological analysis at the population level, it delineates environmental risks on a regional scale rather than quantifying individual exposure levels; consequently, caution must be exercised during result interpretation to avoid the ecological fallacy. Finally, due to limitations in data availability, the model did not directly incorporate key biological and social determinants such as rodent host density and vaccination coverage; consequently, relying solely on demographic and natural environmental variables as indirect proxies may not fully capture the complex transmission mechanisms at a micro-scale.

Conclusions

Hemorrhagic Fever with Renal Syndrome (HFRS) remains a significant natural focal disease posing a threat to public health in Southwest China. Based on the Maximum Entropy (MaxEnt) model, this study systematically characterized the potential geographical distribution patterns and key driving mechanisms of HFRS across the region at a regional scale. Our findings demonstrate that HFRS prevalence is driven by the dual influence of natural environmental factors and anthropogenic activities. Specifically, human population density emerged as the primary predictor, highlighting the amplification effect of human activities on transmission risk, whereas natural variables such as vegetation indices, temperature, and topography constrained the spatial boundaries of natural foci through non-linear mechanisms. The risk prediction maps constructed in this study provide visually intuitive decision-making support for regional public health authorities. We recommend a strategic transition in future prevention and control measures from traditional blanket approaches to precision control, prioritizing strengthened active surveillance in the fringe areas of the Chengdu-Chongqing urban agglomeration, mountainous terraced agricultural zones, and major infrastructure development sites, alongside the

implementation of seasonally differentiated rodent control and vaccination interventions to effectively curb the transmission and spread of the epidemic.

Declarations

Ethics approval and consent to participate

This study did not involve any human intervention or clinical trials. The use of hemorrhagic fever with renal syndrome (HFRS) case data was based on routine public health surveillance activities in China. According to national regulations, such surveillance data are exempt from institutional ethics review. Therefore, ethics approval was not required for this study. As all data were anonymized and contained no personal identifiers or private health information, the requirement for informed consent was also deemed unnecessary. This study was conducted in accordance with the principles of the Declaration of Helsinki.

Consent for publication

Not applicable.

Competing interests

The authors declare that they have no competing interests.

Funding

The authors declare that they have no funding support for this work.

Author Contribution

QC,YX, and WZ conceived and designed the study. DZ, ZZ, and YW collected and organized the data. LZ, Z Zheng, RQ, and FS analyzed the data. DZ wrote the original draft of the manuscript. QC,YX, and WZ reviewed and edited the manuscript. All authors read and approved the final manuscript.

Acknowledgements

Not applicable.

Data Availability

The datasets used and/or analyzed during the current study are available from the corresponding author on reasonable request.

References

1. Glass GE, Shields T, Cai B, Yates TL, Parmenter R. Persistently highest risk areas for hantavirus pulmonary syndrome: potential sites for refugia. Ecol Appl Publ Ecol Soc Am. 2007;17:129–39. https://doi.org/10.1890/1051-0761(2007)017%5B0129:phrafh%5D2.0.co;2
2. Lu W, Kuang L, Hu Y, Shi J, Li Q, Tian W. Epidemiological and clinical characteristics of death from hemorrhagic fever with renal syndrome: A meta-analysis. Front Microbiol. 2024;15:1329683. https://doi.org/10.3389/fmicb.2024.1329683
3. Tkachenko E, Kurashova S, Balkina A, Ivanov A, Egorova M, Leonovich O, et al. Cases of hemorrhagic fever with renal syndrome in Russia during 2000–2022. Viruses. 2023;15:1537. https://doi.org/10.3390/v15071537
4. Prayitno SP, Natasha A, Lee S, Kim C-M, Lee YM, Park K, et al. Etiological agent and clinical characteristics of haemorrhagic fever with renal syndrome in the southern republic of korea: a genomic surveillance study. Clin Microbiol Infect Off Publ Eur Soc Clin Microbiol Infect Dis. 2024;30:795–802. https://doi.org/10.1016/j.cmi.2024.02.014
5. Avšič-Županc T, Saksida A, Korva M. Hantavirus infections. Clin Microbiol Infect Off Publ Eur Soc Clin Microbiol Infect Dis. 2019;21S:e6–16. https://doi.org/10.1111/1469-0691.12291
6. Bai X-H, Peng C, Jiang T, Hu Z-M, Huang D-S, Guan P. Distribution of geographical scale, data aggregation unit and period in the correlation analysis between temperature and incidence of HFRS in mainland China: A systematic review of 27 ecological studies. PLoS Negl Trop Dis. 2019;13:e0007688. https://doi.org/10.1371/journal.pntd.0007688
7. Wang Y, Zhang C, Gao J, Chen Z, Liu Z, Huang J, et al. Spatiotemporal trends of hemorrhagic fever with renal syndrome (HFRS) in China under climate variation. Proc Natl Acad Sci. Proceedings of the National Academy of Sciences; 2024;121:e2312556121. https://doi.org/10.1073/pnas.2312556121
8. Zheng Z, Li Z, Huang X, Wang Q, Du S, Li A, et al. Hemorrhagic fever with renal syndrome and diversity and distribution of hantaviruses — China, 2014–2023. China CDC Wkly. 2025;7:858–62. https://doi.org/10.46234/ccdcw2025.141
9. Wei Q, Ren H, Lu L, Shi R. Non-negligible impacts of urbanization on spatiotemporal variations of infectious disease: A case study of hemorrhagic fever with renal syndrome epidemics in China. Infect Dis Poverty. 2025;14:104. https://doi.org/10.1186/s40249-025-01366-w
10. Guo X, Li R, Li Y, Tian X, Gao Y, Yu L, et al. Meteorological drivers of hemorrhagic fever with renal syndrome in China's jiaodong peninsula: An ecological time-series study from 2020 to 2024. Front Public Health. 2025;13:1743845. https://doi.org/10.3389/fpubh.2025.1743845
11. Wang Y, Wei X, Jia R, Peng X, Zhang X, Yang M, et al. The spatiotemporal pattern and its determinants of hemorrhagic fever with renal syndrome in northeastern China: Spatiotemporal analysis. JMIR Public Health Surveill. 2023;9:e42673. https://doi.org/10.2196/42673

12. Sipari S, Khalil H, Magnusson M, Evander M, Hörnfeldt B, Ecke F. Climate change accelerates winter transmission of a zoonotic pathogen. Ambio. 2022;51:508–17. https://doi.org/10.1007/s13280-021-01594-y
13. Wang Y, Wei X, Xiao X, Yin W, He J, Ren Z, et al. Climate and socio-economic factors drive the spatio-temporal dynamics of HFRS in northeastern China. One Health. Amsterdam, Netherlands; 2022;15:100466. https://doi.org/10.1016/j.onehlt.2022.100466
14. Song W-Y, Lv Y, Yin P-W, Yang Y-Y, Guo X-G. Potential distribution of leptotrombidium scutellare in yunnan and sichuan provinces, China, and its association with mite-borne disease transmission. Parasit Vectors. 2023;16:164. https://doi.org/10.1186/s13071-023-05789-y
15. Wang N, Yin J-X, Zhang Y, Wu L, Li W-H, Luo Y-Y, et al. Genetic evolution analysis and host characteristics of hantavirus in yunnan province, China. Int J Environ Res Public Health. 2022;19:13433. https://doi.org/10.3390/ijerph192013433
16. Zhang Y, Geng M, Shi Y, Jin B, Xiong Q, Zhou S, et al. Epidemiological characteristics and trends of zoonotic diseases in China from 2015 to 2022. Trop Med Infect Dis. 2025;10:159. https://doi.org/10.3390/tropicalmed10060159
17. Chen T, Chen J, Wei X, Yang S, Li Y, Yuan Y, et al. Quantifying the contributions of climate change and human activities to grassland dynamics in southwest of China using a spatiotemporally varying residual method. Int J Digit Earth. Taylor & Francis; 2025;18:2484473. https://doi.org/10.1080/17538947.2025.2484473
18. Yang S, Liu J, Song J. [seroepidemiologic study on hemorrhagic fever with renal syndrome virus in the migration areas of the three-gorges reservoir chongqing, region, yangtze river]. Zhonghua Liu Xing Bing Xue Za Zhi Zhonghua Liuxingbingxue Zazhi. 2001;22:284–6.
19. Song W-Y, Lv Y, Yin P-W, Yang Y-Y, Guo X-G. Potential distribution of leptotrombidium scutellare in yunnan and sichuan provinces, China, and its association with mite-borne disease transmission. Parasit Vectors. 2023;16:164. https://doi.org/10.1186/s13071-023-05789-y
20. Chang ZR, Lu L, Mao DQ, Pan HM, Feng LG, Yang XB, et al. Dynamics of rodent and rodent-borne disease during construction of the three gorges reservoir from 1997 to 2012. Biomed Environ Sci BES. 2016;29:197–204. https://doi.org/10.3967/bes2016.024
21. Li H, Yang R, Guan X, Huang X, Jiang H, Tan L, et al. Spatiotemporal distribution and meteorological factors of hemorrhagic fever with renal syndrome in hubei province. PLoS Negl Trop Dis. 2024;18:e0012498. https://doi.org/10.1371/journal.pntd.0012498
22. Bai Y, Xu Z, Lu B, Sun Q, Tang W, Liu X, et al. Effects of climate and rodent factors on hemorrhagic fever with renal syndrome in chongqing, China, 1997–2008. PLOS One. 2015;10:e0133218. https://doi.org/10.1371/journal.pone.0133218
23. Zou Y, Hu J, Wang Z-X, Wang D-M, Li M-H, Ren G-D, et al. Molecular diversity and phylogeny of hantaan virus in guizhou, China: Evidence for guizhou as a radiation center of the present hantaan virus. J Gen Virol. 2008;89:1987–97. https://doi.org/10.1099/vir.0.2008/000497-0

24. Huang H, Fu M, Han P, Yin H, Yang Z, Kong Y, et al. Clinical and molecular epidemiology of hemorrhagic fever with renal syndrome caused by orthohantaviruses in xiangyun county, dali prefecture, yunnan province, China. Vaccines. 2023;11:1477. https://doi.org/10.3390/vaccines11091477
25. Ministry of Health of the People's Republic of China. Diagnostic criteria for epidemic hemorrhagic fever (WS 278–2008). Beijing: Ministry of Health of the People's Republic of China; 2008.
26. Restrepo AMC, Martin BM, Fuimaono S, Clements ACA, Graves PM, Lau CL. Spatial predictive risk mapping of lymphatic filariasis residual hotspots in American samoa using demographic and environmental factors. PLoS Negl Trop Dis. Public Library of Science; 2023;17:e0010840. https://doi.org/10.1371/journal.pntd.0010840
27. Wang R, Yang H, Luo W, Wang M, Lu X, Huang T, et al. Predicting the potential distribution of the asian citrus psyllid, diaphorina citri (kuwayama), in China using the MaxEnt model. PeerJ. PeerJ Inc.; 2019;7:e7323. https://doi.org/10.7717/peerj.7323
28. Conley AK, Fuller DO, Haddad N, Hassan AN, Gad AM, Beier JC. Modeling the distribution of the west nile and rift valley fever vector culex pipiens in arid and semi-arid regions of the middle east and north africa. Parasit Vectors. 2014;7:289. https://doi.org/10.1186/1756-3305-7-289
29. Kong F, Tang L, He H, Yang F, Tao J, Wang W. Assessing the impact of climate change on the distribution of osmanthus fragrans using maxent. Environ Sci Pollut Res. 2021;28:34655–63. https://doi.org/10.1007/s11356-021-13121-3
30. Fan S, Chen C, Zhao Q, Wei J, Zhang H, Fan S, et al. Identifying potentially climatic suitability areas for arma custos (hemiptera: Pentatomidae) in China under climate change. Insects [Internet]. 2020 [cited 2026 Jan 12];11. https://doi.org/10.3390/insects11100674
31. Lee CM, Lee D-S, Kwon T-S, Athar M, Park Y-S, Lee CM, et al. Predicting the global distribution of solenopsis geminata (hymenoptera: Formicidae) under climate change using the MaxEnt model. Insects [Internet]. 2021 [cited 2026 Jan 12];12. https://doi.org/10.3390/insects12030229
32. Pramanik M, Singh P, Dhiman RC. Identification of bio-climatic determinants and potential risk areas for kyasanur forest disease in southern India using MaxEnt modelling approach. BMC Infect Dis. 2021;21:1226. https://doi.org/10.1186/s12879-021-06908-9
33. Slater H, Michael E. Predicting the current and future potential distributions of lymphatic filariasis in africa using maximum entropy ecological niche modelling. PLOS ONE. Public Library of Science; 2012;7:e32202. https://doi.org/10.1371/journal.pone.0032202
34. Zhang J, Jiang F, Li G, Qin W, Li S, Gao H, et al. Maxent modeling for predicting the spatial distribution of three raptors in the sanjiangyuan national park, China. Ecol Evol. 2019;9:6643–54. https://doi.org/10.1002/ece3.5243
35. Anand V, Oinam B, Singh IH. Predicting the current and future potential spatial distribution of endangered rucervus eldii eldii (sangai) using MaxEnt model. Environ Monit Assess. 2021;193:147. https://doi.org/10.1007/s10661-021-08950-1

36. Holcomb KM, Nguyen C, Foy BD, Ahn M, Cramer K, Lonstrup ET, et al. Effects of ivermectin treatment of backyard chickens on mosquito dynamics and west nile virus transmission. PLoS Negl Trop Dis. Public Library of Science; 2022;16:e0010260. https://doi.org/10.1371/journal.pntd.0010260
37. Acharya BK, Cao C, Xu M, Khanal L, Naeem S, Pandit S, et al. Present and future of dengue fever in nepal: Mapping climatic suitability by ecological niche model. Int J Environ Res Public Health [Internet]. 2018 [cited 2026 Jan 12];15. https://doi.org/10.3390/ijerph15020187
38. Glass GE. Forecasting outbreaks of hantaviral disease: future directions in geospatial modeling. Viruses. 2023;15:1461. https://doi.org/10.3390/v15071461
39. He J, Christakos G, Wu J, Jankowski P, Langousis A, Wang Y, et al. Probabilistic logic analysis of the highly heterogeneous spatiotemporal HFRS incidence distribution in heilongjiang province (China) during 2005–2013. PLoS Negl Trop Dis. 2019;13:e0007091. https://doi.org/10.1371/journal.pntd.0007091
40. He J, Wang Y, Wei X, Sun H, Xu Y, Yin W, et al. Spatial-temporal dynamics and time series prediction of HFRS in mainland China: A long-term retrospective study. J Med Virol. 2023;95:e28269. https://doi.org/10.1002/jmv.28269
41. Guo X, Li R, Li Y, Tian X, Gao Y, Yu L, et al. Meteorological drivers of hemorrhagic fever with renal syndrome in China's jiaodong peninsula: An ecological time-series study from 2020 to 2024. Front Public Health. 2025;13:1743845. https://doi.org/10.3389/fpubh.2025.1743845
42. Wang Y, Wei X, Xiao X, Yin W, He J, Ren Z, et al. Climate and socio-economic factors drive the spatio-temporal dynamics of HFRS in northeastern China. One Health Amst Neth. 2022;15:100466. https://doi.org/10.1016/j.onehlt.2022.100466
43. Li S, Zhu L, Zhang L, Zhang G, Ren H, Lu L. Urbanization-related environmental factors and hemorrhagic fever with renal syndrome: A review based on studies taken in China. Int J Environ Res Public Health. 2023;20:3328. https://doi.org/10.3390/ijerph20043328
44. Wang Y, Zhang C, Gao J, Chen Z, Liu Z, Huang J, et al. Spatiotemporal trends of hemorrhagic fever with renal syndrome (HFRS) in China under climate variation. Proc Natl Acad Sci U S A. 121:e2312556121. https://doi.org/10.1073/pnas.2312556121
45. Wei Q, Ren H, Lu L, Shi R. Non-negligible impacts of urbanization on spatiotemporal variations of infectious disease: a case study of hemorrhagic fever with renal syndrome epidemics in China. Infect Dis Poverty. 2025;14:104. https://doi.org/10.1186/s40249-025-01366-w
46. Li ZL, Ping LY, Liang LU, Juan LS, Yan RH. Spatial heterogeneity and influencing factors of HFRS epidemics in rural and urban areas: A study in guanzhong plain of shaanxi province, China. Biomed Environ Sci. 2022;35:1012–24. https://doi.org/10.3967/bes2022.130
47. Clay CA, Lehmer EM, St Jeor S, Dearing MD. Testing mechanisms of the dilution effect: Deer mice encounter rates, sin nombre virus prevalence and species diversity. Ecohealth. 2009;6:250–9. https://doi.org/10.1007/s10393-009-0240-2
48. Liu Y, Liu C, Wang L, Chen X, Qiao H, Zhang Y, et al. Investigating the impact of climatic and environmental factors on HFRS prevalence in anhui province, China, using satellite and reanalysis

data. Front Public Health [Internet]. Frontiers; 2024 [cited 2026 Jan 13];12. https://doi.org/10.3389/fpubh.2024.1447501

49. Li L, Wang C-H, Wang S-F, Li M-T, Yakob L, Cazelles B, et al. Hemorrhagic fever with renal syndrome in China: mechanisms on two distinct annual peaks and control measures.:1–22. https://doi.org/10.1142/S1793524518500304
50. Wang Y, Zhang C, Gao J, Chen Z, Liu Z, Huang J, et al. Spatiotemporal trends of hemorrhagic fever with renal syndrome (HFRS) in China under climate variation. Proc Natl Acad Sci. Proceedings of the National Academy of Sciences; 2024;121:e2312556121. https://doi.org/10.1073/pnas.2312556121
51. Chang N, Huang W, Niu Y, Xu Z, Gao Y, Ye T, et al. Risk of hemorrhagic fever with renal syndrome associated with meteorological factors in diverse epidemic regions: a nationwide longitudinal study in China. Infect Dis Poverty. 2025;14:3. https://doi.org/10.1186/s40249-024-01272-7
52. He J, Wang Y, Wei X, Sun H, Xu Y, Yin W, et al. Spatial-temporal dynamics and time series prediction of HFRS in mainland China: A long-term retrospective study. J Med Virol. 2023;95:e28269. https://doi.org/10.1002/jmv.28269
53. Wang Y, Wei X, Xiao X, Yin W, He J, Ren Z, et al. Climate and socio-economic factors drive the spatio-temporal dynamics of HFRS in northeastern China. One Health. 2022;15:100466. https://doi.org/10.1016/j.onehlt.2022.100466
54. Sun W, Liu X, Li W, Mao Z, Sun J, Lu L. Effects and interaction of meteorological factors on hemorrhagic fever with renal syndrome incidence in huludao city, northeastern China, 2007–2018. PLoS Negl Trop Dis. 2021;15:e0009217. https://doi.org/10.1371/journal.pntd.0009217
55. Luo Y, Lv H, Yan H, Zhu C, Ai L, Li W, et al. Meteorological change and hemorrhagic fever with renal syndrome epidemic in China, 2004–2018. Sci Rep. 2022;12:20037. https://doi.org/10.1038/s41598-022-23945-9
56. Wen B, Yang Z, Ren S, Fu T, Li R, Lu M, et al. Spatial-temporal patterns and influencing factors for hemorrhagic fever with renal syndrome: A 16-year national surveillance analysis in China. One Health. 2024;18:100725. https://doi.org/10.1016/j.onehlt.2024.100725
57. Fang L-Q, Wang X-J, Liang S, Li Y-L, Song S-X, Zhang W-Y, et al. Spatiotemporal trends and climatic factors of hemorrhagic fever with renal syndrome epidemic in shandong province, China. PLoS Negl Trop Dis. 2010;4:e789. https://doi.org/10.1371/journal.pntd.0000789
58. Xiao H, Tian H-Y, Gao L-D, Liu H-N, Duan L-S, Basta N, et al. Animal reservoir, natural and socioeconomic variations and the transmission of hemorrhagic fever with renal syndrome in chenzhou, China, 2006–2010. PLoS Negl Trop Dis. Public Library of Science; 2014;8:e2615. https://doi.org/10.1371/journal.pntd.0002615
59. Zhao Y, Ge L, Liu J, Liu H, Yu L, Wang N, et al. Analyzing hemorrhagic fever with renal syndrome in hubei province, China: A space-time cube-based approach. J Int Med Res. 2019;47:3371–88. https://doi.org/10.1177/0300060519850734
60. Ye S, Ren S, Song C, Du Z, Wang K, Du B, et al. Spatial pattern of cultivated land fragmentation in mainland China: Characteristics, dominant factors, and countermeasures. Land Use Policy.

2024;139:107070. https://doi.org/10.1016/j.landusepol.2024.107070

61. Xiao H, Tong X, Huang R, Gao L, Hu S, Li Y, et al. Landscape and rodent community composition are associated with risk of hemorrhagic fever with renal syndrome in two cities in China, 2006–2013. BMC Infect Dis. 2018;18:37. https://doi.org/10.1186/s12879-017-2827-5
62. M Y, Y L. Agroecosystem composition and landscape ecological risk evolution of rice terraces in the southern mountains, China. 2022 [cited 2026 Jan 15]; https://doi.org/10.1016/j.ecolind.2022.109625
63. Zheng X, Wu J, Deng H, Zheng X, Wu J, Deng H. Spatial distribution and land use of traditional villages in southwest China. Sustainability [Internet]. 2021 [cited 2026 Jan 13];13. https://doi.org/10.3390/su13116326
64. Li Z, Xie X, Yan X, Bai T, Xu D. Impact of China's Rural Land Marketization on Ecological Environment Quality Based on Remote Sensing. Int J Environ Res Public Health. 2022;19:12619. https://doi.org/10.3390/ijerph191912619
65. He J, Wang Y, Xu X, Christakos G, Zhang D, Xu Y, et al. Urbanization influences hemorrhagic fever with renal syndrome transmission: 34-year evidence from China's national surveillance. Infect Dis Model. 2026;11:575–85. https://doi.org/10.1016/j.idm.2025.12.004
66. Li S, Zhu L, Zhang L, Zhang G, Ren H, Lu L, et al. Urbanization-related environmental factors and hemorrhagic fever with renal syndrome: A review based on studies taken in China. Int J Environ Res Public Health [Internet]. 2023 [cited 2026 Jan 13];20. https://doi.org/10.3390/ijerph20043328
67. Chang ZR, Lu L, Mao DQ, Pan HM, Feng LG, Yang XB, et al. Dynamics of rodent and rodent-borne disease during construction of the three gorges reservoir from 1997 to 2012. Biomed Environ Sci BES. 2016;29:197–204. https://doi.org/10.3967/bes2016.024
68. Zuo L, Wang H, Tan Y, Wan J, Tan W, Gan Y, et al. Co-circulation of hantavirus, pathogenic leptospira spp., and bartonella spp. in rodents in the wanzhou section of the three gorges reservoir region, 2021–2023. Vector Borne Zoonotic Dis Larchmt N. 2024;24:694–8. https://doi.org/10.1089/vbz.2023.0150
69. Zhang X, Peng L, Liu W, Fan L, Zhang Q, Chen G, et al. Response of primary vectors and related diseases to impoundment by the three gorges dam. Trop Med Int Health TM IH. 2014;19:440–9. https://doi.org/10.1111/tmi.12272
70. Zhou J-H, Zhang H-L, Wang J-L, Yang W-H, Mi Z-Q, Zhang Y-Z, et al. [survey on host animal and molecular epidemiology of hantavirus in chuxiong prefecture, yunnan province]. Zhonghua Liu Xing Bing Xue Za Zhi Zhonghua Liuxingbingxue Zazhi. 2009;30:239–42.
71. Lv Y, Guo X-G, Yin P-W, Huang X-B, Qian T-J. Distribution and infestation of leptotrombidium scutellare (a major vector of scrub typhus) on small mammals across five provincial regions of southwest China. Vet Res Commun. 2025;49:246. https://doi.org/10.1007/s11259-025-10817-6

Figures

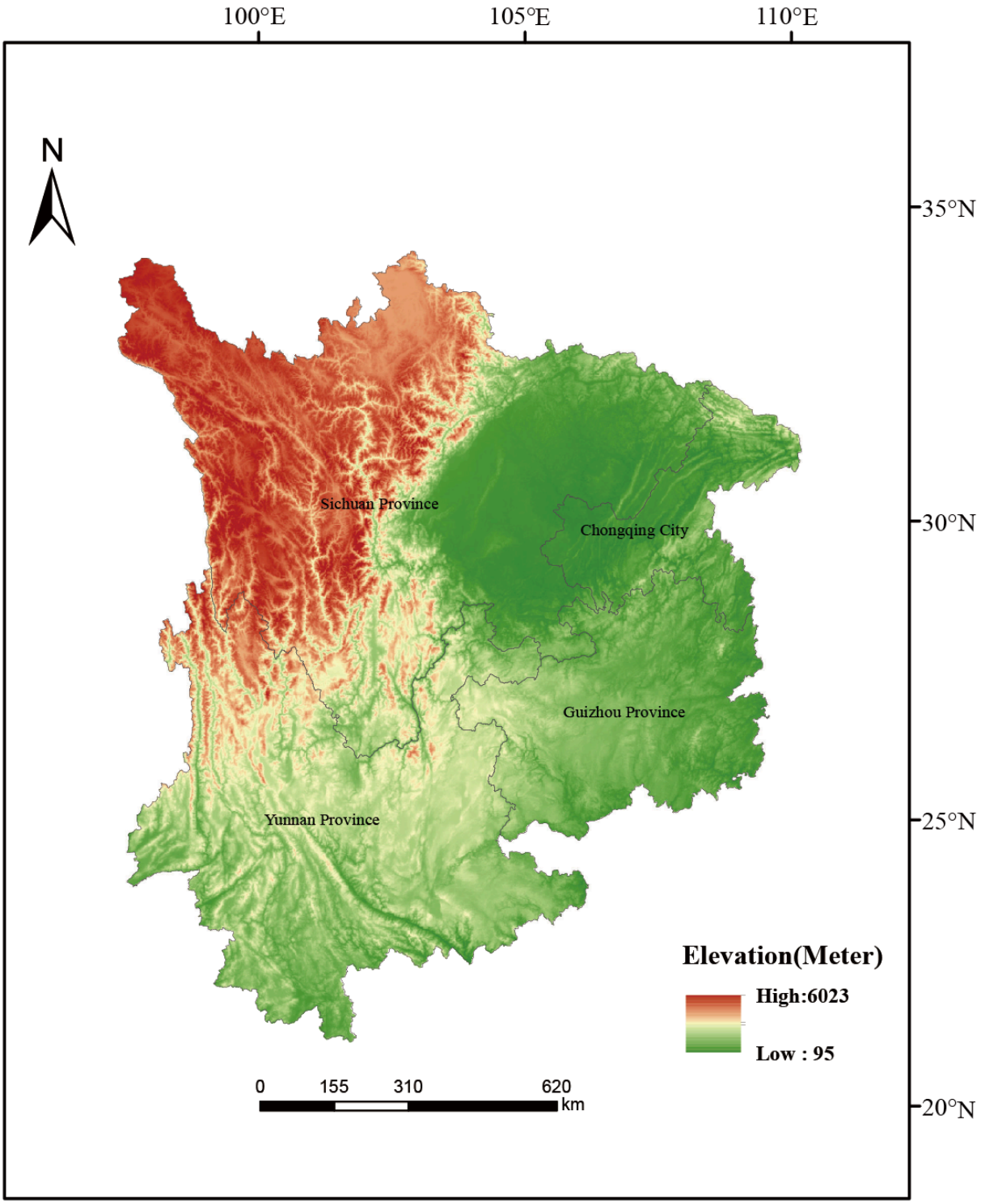


Figure 1

Map of the study area. The figure illustrates the geographical location and elevation gradient of Southwest China.

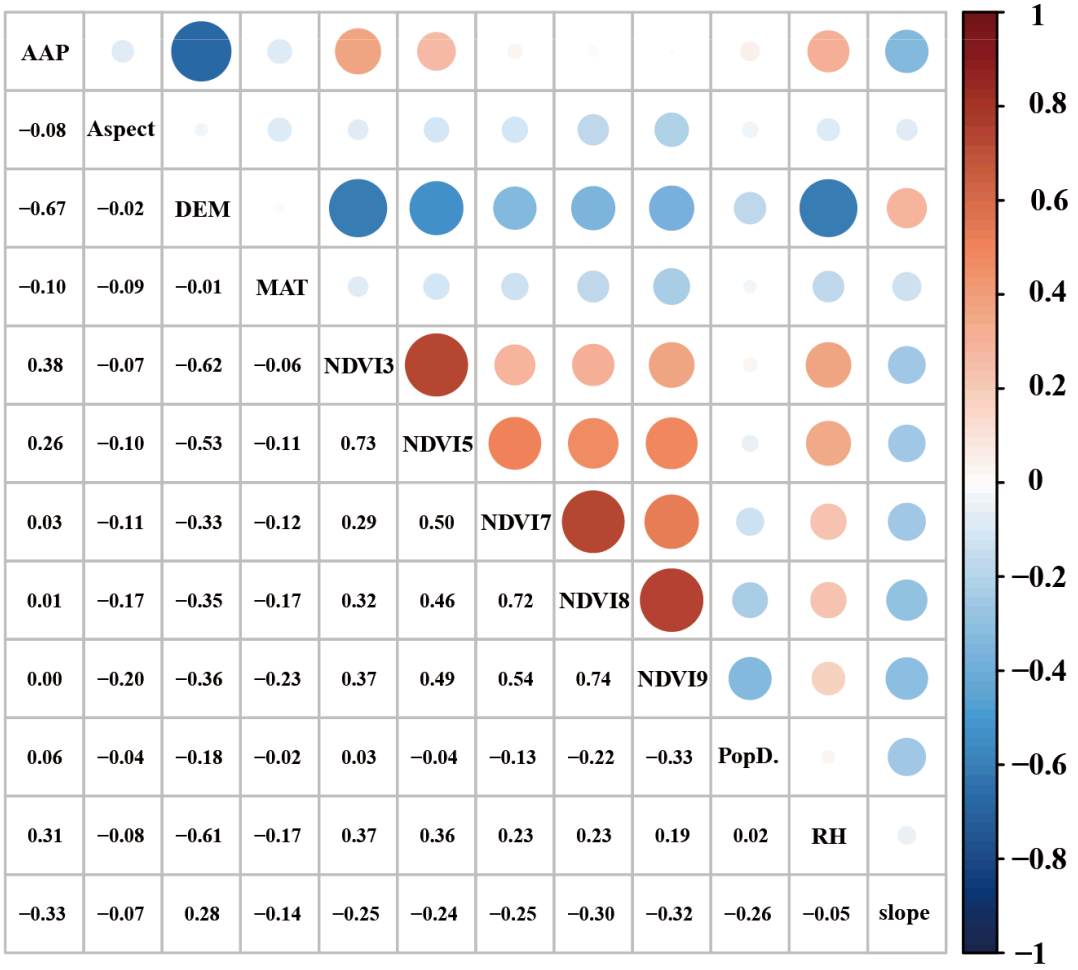


Figure 2

Displays a heatmap illustrating the pairwise Pearson correlation coefficients among different environmental variables in Southwest China.

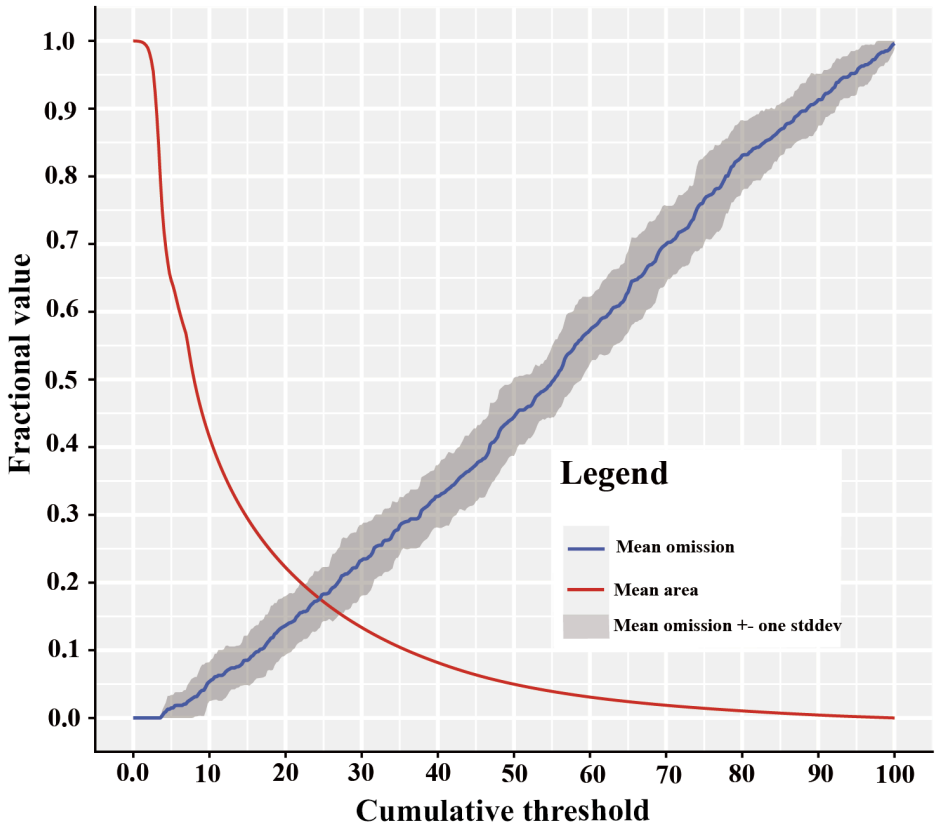


Figure 3

Averaged omission and predicted area for the MaxEnt model of HFRS in Southwest China.

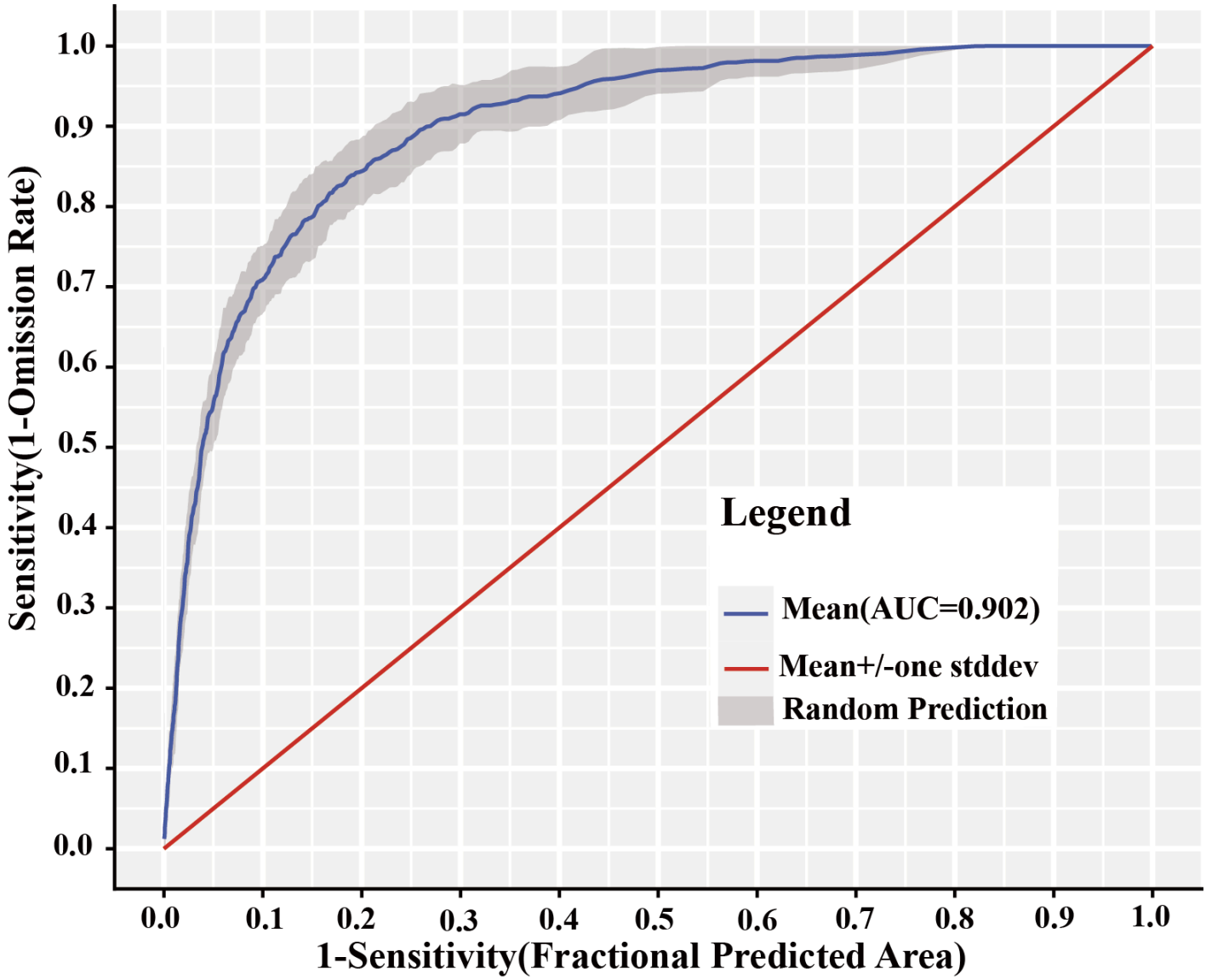


Figure 4

Receiver operating characteristic (ROC) curve for the MaxEnt model of HFRS in Southwest China.

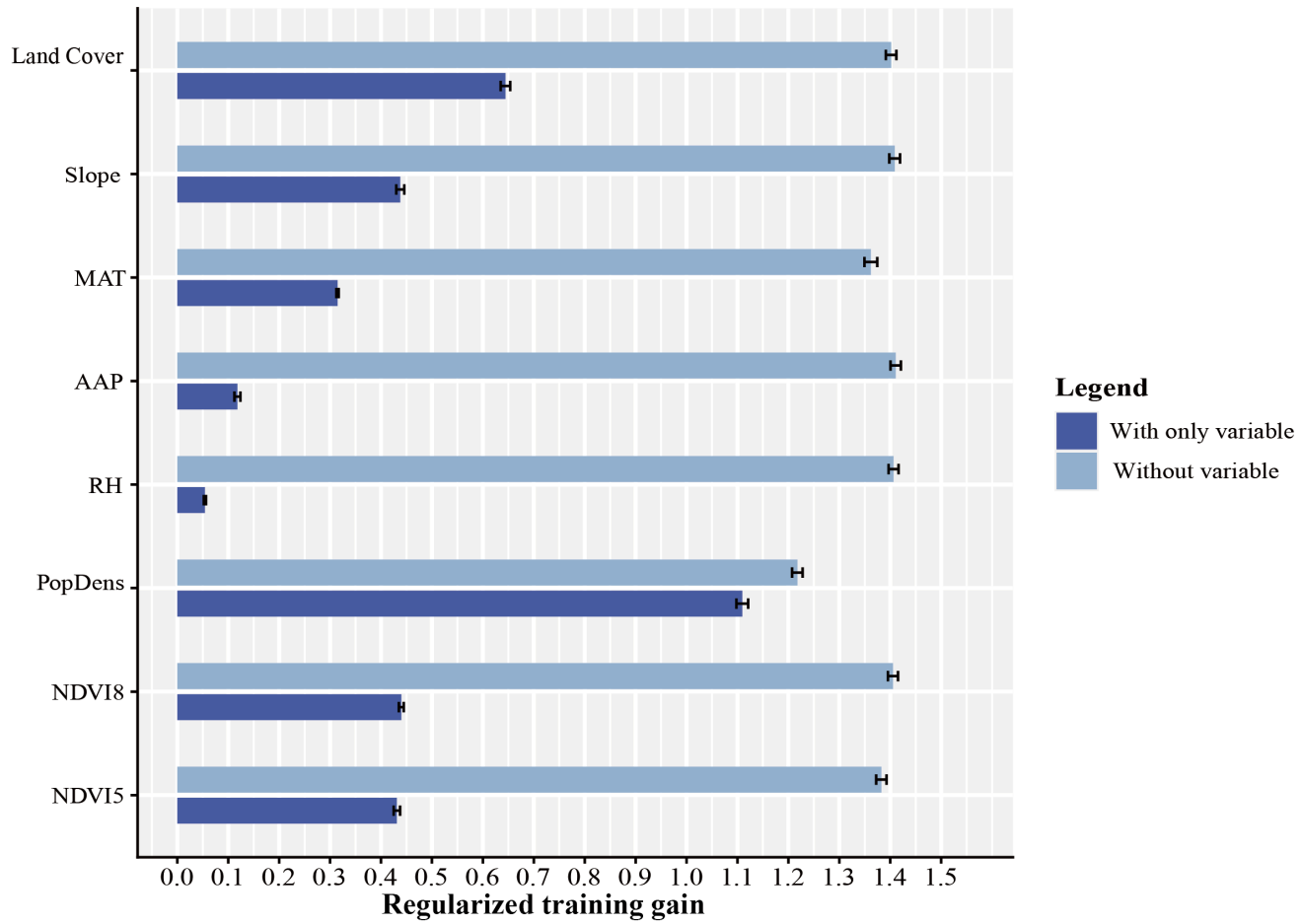


Figure 5

Results of the Jackknife test evaluating the relative importance of predictor variables to the HFRS risk prediction in Southwest China.

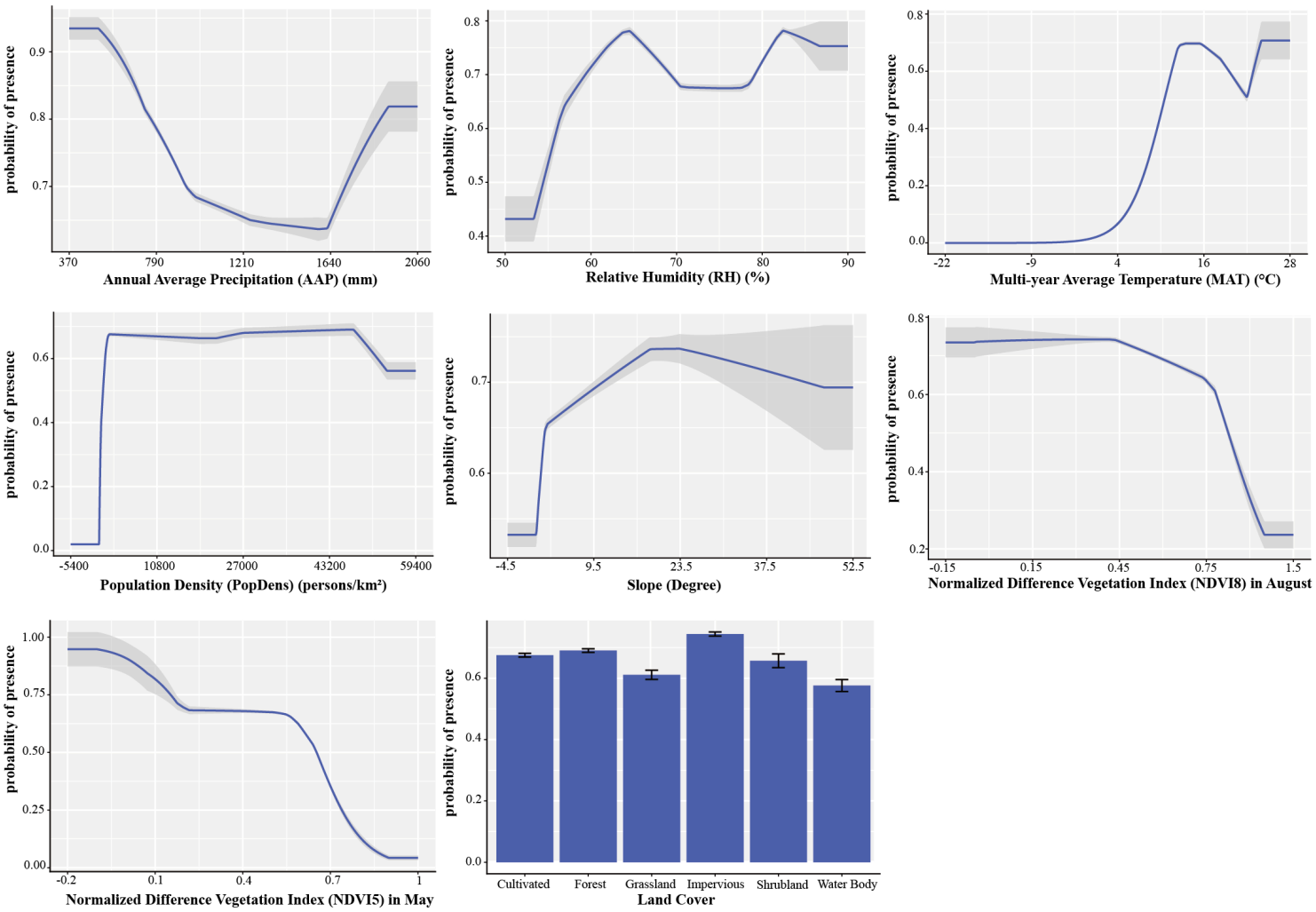


Figure 6

Response curves for the probability of HFRS presence. The curves illustrate the mean response of 10 replicate MaxEnt runs (blue) and the mean ± one standard deviation (grey). The x-axis represents the value of each predictor variable, while the y-axis represents the predicted probability of HFRS occurrence.

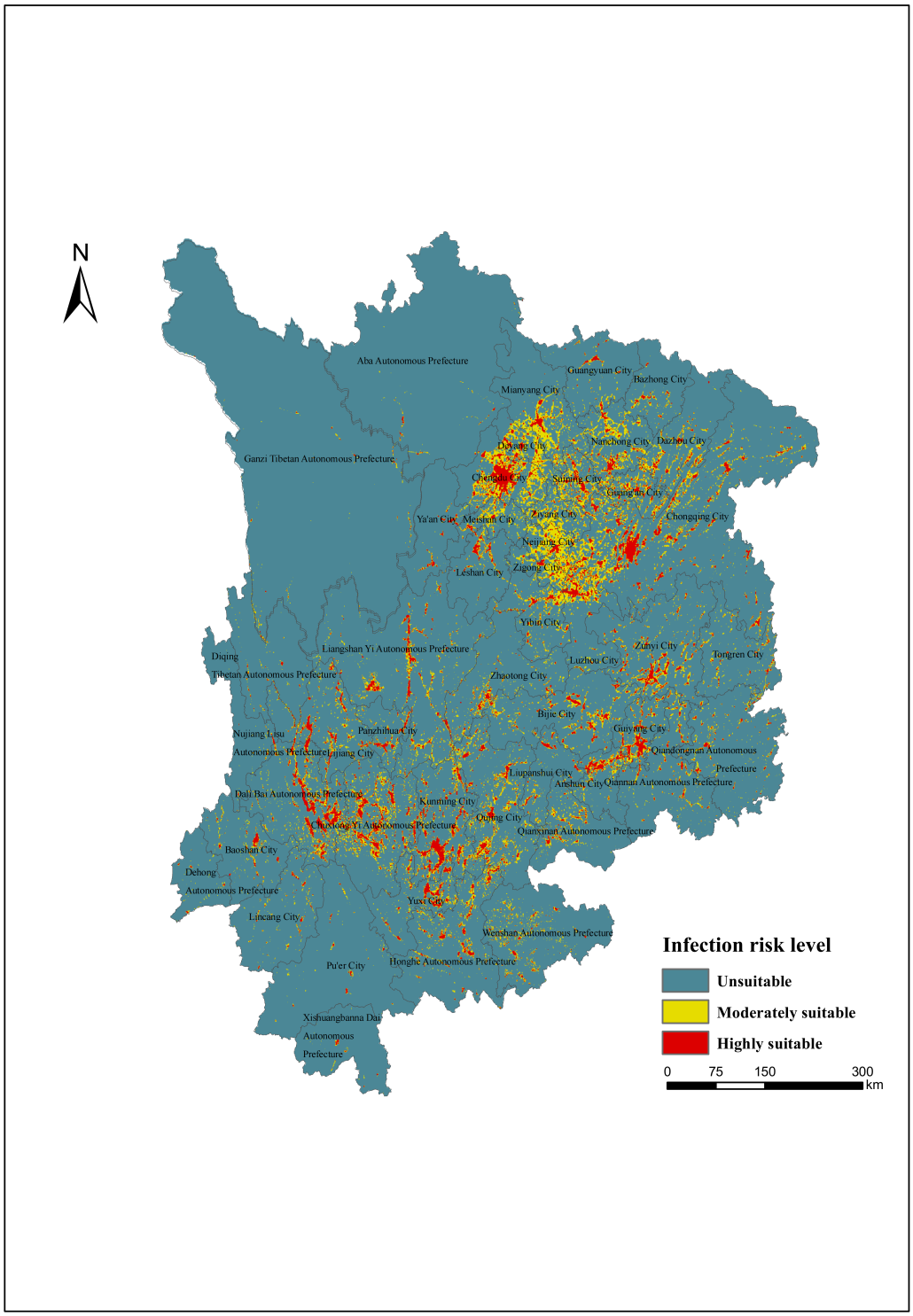


Figure 7

Environmental suitability maps for HFRS in Southwest China.